

AN ADAPTIVE MESH-BASED METHOD FOR THE EFFICIENT SIMULATION OF LSC-DRIVEN MICROBUNCHING GAIN IN FEL APPLICATIONS

Ph. Amstutz*, Universität Hamburg, Hamburg, Germany
M. Vogt, Deutsches Elektronen-Synchrotron DESY, Hamburg, Germany

Abstract

Electron beams with high peak current as they are required for the operation of free-electron lasers (FELs) are often generated by means of a series of magnetic bunch compressors. In conjunction with a collective coherent force, e.g. longitudinal space-charge (LSC), bunch compressors can possibly cause a wavelength dependent amplification of initial density inhomogeneities, potentially to an extent detrimental to the operation of the FEL. A common model, consisting of LSC, acceleration (kicks), and magnetic chicanes (drift-type maps), is governed by a time-discrete Vlasov-Poisson system. Such systems have been successfully simulated using mesh based representations of the phase space density (PSD) and the method of characteristics for the update step. However, for the irregular and exotic PSDs, prevalent in FEL applications, a homogeneous high resolution discretization on a naive rectangular mesh can be prohibitively wasteful. Here we present an approach based on adaptive tree refinement that addresses the complexity of the PSDs and allows for the efficient simulation of LSC-driven micro-bunching in FELs.

INTRODUCTION

The operational principle of free-electron lasers relies on high brightness electron bunches driving the photon energy gain process. Bunches featuring the required peak current cannot be produced from the gun directly but have to be generated by the method of bunch compression. The bunch is prepared with an energy chirp during acceleration in RF-cavities operated at an off-crest phase. Then, due to the energy dependent path length in a magnetic chicane the bunch is longitudinally compressed. Usually this process is repeated multiple times during the acceleration process. It became apparent that such compression schemes can give rise to an enhancement of initially existing longitudinal density inhomogeneities in the bunch, an effect known as micro-bunching [1–4]. In the linear accelerator part of a bunch compression stage the electrons inside the bunch interact with the electric self-field resulting from their inhomogeneous distribution. This leads to a to a position dependent variation of the electron energy and hence to the introduction of (additional) energy inhomogeneities. In the following magnetic chicane the change of an electron's longitudinal position is related to its energy, so that the overall influence of a bunch compressor can indeed lead to an amplification or damping of a preexisting current modulation.

The longitudinal dynamics of the electron bunch are governed by the Vlasov-Poisson equation. In the ultra-relativistic limit, and under the assumption that the magnetic chicane is much shorter than the linear accelerator part and hence neglecting energy variations due to LSC within it, an exactly time-discrete model exists. The model [3] does explicitly not include coherent synchrotron radiation (CSR). The time evolution of a PSD within this model can therefore be simulated by tracking it over the intrinsically discrete (and long) time steps without the need for optimized step-sizes.

In this contribution we present the foundations for and the present status of a computer code based on the Perron-Frobenius method [5, 6] that is currently under development.

PERRON-FROBENIUS OPERATOR

In a Hamiltonian system with N degrees of freedom the time evolution of a phase-space vector $\vec{z} = (q^1, p^1, \dots, q^N, p^N)$ between two points in time t_0 and t_1 is given by a symplectic map, $\vec{M}_{1 \leftarrow 0} : \mathbb{R}^{2N} \rightarrow \mathbb{R}^{2N}$, so that

$$\vec{z}_1 = \vec{M}_{1 \leftarrow 0}(\vec{z}_0), \quad (1)$$

where $\vec{z}_i = \vec{z}|_{t=t_i}$. It can be shown that symplectic maps are volume preserving, $d\vec{z}_1 = d\vec{z}_0$. Conservation of probability dictates that during the time evolution of a phase-space distribution $\Psi : \mathbb{R}^{2N} \rightarrow \mathbb{R}$ the integrated phase-space distribution within a volume element $d\vec{z}$ is constant,

$$\Psi_1(\vec{z}_1) d\vec{z}_1 = \Psi_0(\vec{z}_0) d\vec{z}_0,$$

where $\Psi_i = \Psi|_{t=t_i}$. Under volume preserving maps, this immediately yields a relation between the phase-space distribution at two points in time

$$\Psi_1(\vec{z}_1) = \Psi_0(\vec{z}_0). \quad (2)$$

Hence, we see that the value of a phase-space distribution is constant on trajectories solving the Hamilton equations of motion. As \vec{z}_0 and \vec{z}_1 are connected by a symplectic, hence invertible map from Eq. (1) follows

$$\vec{z}_0 = \vec{M}_{1 \leftarrow 0}^{-1}(\vec{z}_1) =: \vec{M}_{0 \leftarrow 1}(\vec{z}_1).$$

When applied to Eq. (2) this yields

$$\Psi_1(\vec{z}_1) = \Psi_0(\vec{M}_{0 \leftarrow 1}(\vec{z}_1)), \quad (3)$$

The time-forward PSD Ψ_1 is therefore fully defined by an initial PSD Ψ_0 and the symplectic map $\vec{M}_{1 \leftarrow 0}$ connecting the two points in time. This is reflected by the introduction of the

Perron-Frobenius operator $\mathcal{M} : \mathcal{L}_1(\mathbb{R}^{2N}, \mathbb{R}) \rightarrow \mathcal{L}_1(\mathbb{R}^{2N}, \mathbb{R})$ associated to the map \vec{M} , which is defined by its action on a real-valued function g

$$(\mathcal{M}g)(\vec{z}) := g(\vec{M}^{-1}(\vec{z})). \quad (4)$$

Here $\mathcal{L}_1(A, B)$ denotes the Banach space of absolute Lebesgue integrable functions from A to B . In passing we note that the PSDs are elements of the (infinite dimensional) unit sphere in $\mathcal{L}_1(\mathbb{R}^{2N}, \mathbb{R})$. With this Eq. (3) can be rewritten as

$$\Psi_1(\vec{z}) = (\mathcal{M}_{1 \leftarrow 0} \Psi_0)(\vec{z}), \quad (5)$$

or simply $\Psi_1 = \mathcal{M}_{1 \leftarrow 0} \Psi_0$. When describing collective effects \vec{M} and thus \mathcal{M} will depend on the initial phase-space distribution Ψ_0 , so that we arrive at

$$\Psi_1(\vec{z}) = (\mathcal{M}[\Psi_0]_{1 \leftarrow 0} \Psi_0)(\vec{z}), \quad (6)$$

or simply $\Psi_1 = \mathcal{M}[\Psi_0]_{1 \leftarrow 0} \Psi_0$. For time continuous systems this evolution is described by the Vlasov equation $\partial_t \Psi = \{H[\Psi], \Psi\}$. Then the dependence of \vec{M} and \mathcal{M} on Ψ_0 is only formal and makes sense only in the limit of small time steps $t_1 - t_0$. We will see, however, that under the assumptions of our model the discrete-time system becomes exact.

MULTI-STAGE BUNCH COMPRESSION

In order to investigate the influence of multi-stage bunch compression on the longitudinal phase-space distribution of an electron bunch we use a straightforward model for the effects of the involved beam-line elements. In this model [3] a compression stage is thought of as being composed of three distinct elements; a string of RF-cavities increasing the particle's energy, a magnetic chicane causing an energy dependent longitudinal translation, and a drift space connecting both as illustrated in Figure 1. We will see soon that the cavities and the LSC free space drift can in fact be combined. The magnetic chicane is assumed to be much shorter than the linear accelerator part comprising the cavity and the drift space, to the extent that LSC-effects within this region can be neglected. Inside the cavity a particle gains an certain amount of energy which is dependent on its arrival time, which is modeled by a kick-type map

$$K_{\text{cav}} : \begin{pmatrix} q \\ p \end{pmatrix} \rightarrow \begin{pmatrix} q \\ p + \Delta p_{\text{cav}}(q) \end{pmatrix},$$

where q is the particle's longitudinal position relative to the reference particle $q = z - z_0$ and p being the deviation from the reference particle's energy $p = E - E_0$. The path length of a particle in a magnetic chicane is dependent on its energy. Hence, its effect is given by a drift-type map

$$D_{\text{chi}} : \begin{pmatrix} q \\ p \end{pmatrix} \rightarrow \begin{pmatrix} q + \Delta q(p) \\ p \end{pmatrix}.$$

We consider LSC effects only in the drift spaces (and in the cavities). They describe the change of a particle's energy due to interaction with the self-fields generated within the

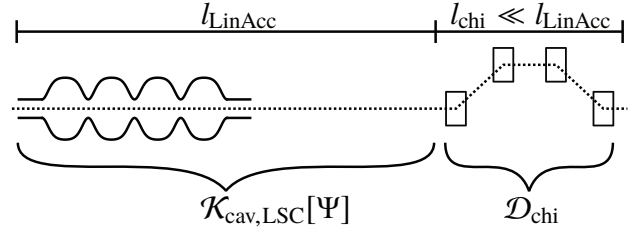


Figure 1: Illustration of the model used for one bunch-compressor stage including the associated Perron-Frobenius operators.

bunch as a result of inhomogeneities in the longitudinal charge density $Q_{\text{bunch}} \rho(q)$. This spatial density is given as the projection of the PSD onto the spatial axis

$$\rho[\Psi](q) = \int_{-\infty}^{\infty} dp \Psi(q, p).$$

The electric self-field in the bunch rest frame and hence the force acting on a particle is, in general, a functional of $\rho(q)$, usually found by solving the appropriate Poisson equation accounting for the transverse shape of the bunch. The resulting force acting on a particle is independent on its energy, so that the LSC effects can be described by the kick-type map

$$K_{\text{LSC}}[\Psi] : \begin{pmatrix} q \\ p \end{pmatrix} \rightarrow \begin{pmatrix} q \\ p + G[\rho](q) \end{pmatrix},$$

where velocity effects are neglected in the ultra-relativistic limit. It is important to note that the spatial density $\rho[\Psi]$ is invariant under kick-type maps,

$$\rho[\Psi_1] = \rho[K_{1 \leftarrow 0} \Psi_0] = \int_{-\infty}^{\infty} dp \Psi(q, p - \Delta p(q)) = \rho[\Psi_0].$$

Because of this invariance the effect of LSC over a finite distance in a non-dispersive section in the beam line can be described by a single, time-discrete Perron-Frobenius step. As can be seen, all maps used in this model are trivially invertible, e.g. the inverse of the combined acceleration and LSC kick is simply

$$K_{\text{cav,LSC}}^{-1}[\Psi] : \begin{pmatrix} q \\ p \end{pmatrix} \rightarrow \begin{pmatrix} q \\ p - G[\rho](q) - \Delta p_{\text{cav}}(q) \end{pmatrix},$$

so that the associated Perron-Frobenius operators $\mathcal{K}_{\text{cav,LSC}}[\Psi]$ and \mathcal{D}_{chi} are easily found. Hence, the phase-space distribution Ψ_n after the n -th bunch-compressor stage is given by

$$\Psi_n = \mathcal{D}_{\text{chi},n-1} \mathcal{K}_{\text{cav,LSC},n-1}[\Psi_{n-1}] \Psi_{n-1}. \quad (7)$$

We note again that the step $n \rightarrow n + 1$ is from one bunch compressor stage to the next.

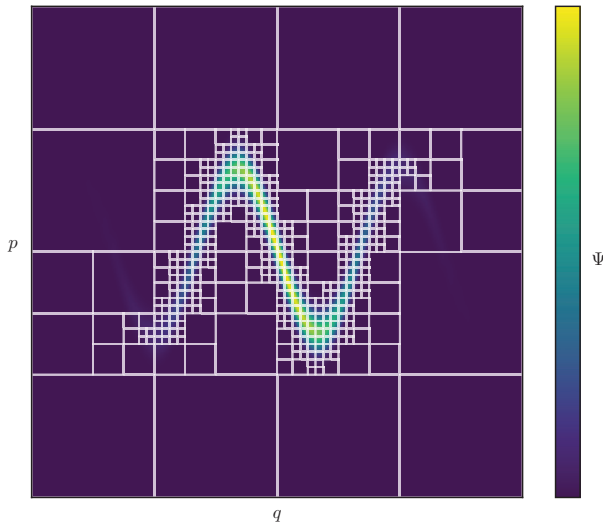


Figure 2: Illustration of the quadtree domain decomposition approach applied to a hypothetical phase-space density with a maximum recursion depth of six.

TREE-BASED MESHING

Electron bunches in FELs often times feature an *exotic* longitudinal phase-space distribution, in the sense that large regions of the phase space are empty whereas most of the probability is confined in a thin, band-like structure. In addition, the expected micro bunching occurs on length scales much shorter than the overall bunch length. For a computer code discretizing the approach (7) this leads to the need for a sophisticated internal representation of the PSDs. The naive approach of sampling the PSDs on a homogeneous mesh spanning a rectangle around the phase-space region of interest and with a resolution high enough to resolve the micro bunching leads to large amounts of memory and computation time being wasted on processing the large regions where effectively $\Psi(q, p) = 0$. To address this problem in our code, we implement the representation of the PSD on an adaptive grid tree, allowing for high resolution in regions where $\Psi(q, p) \neq 0$ while storing the empty regions with only coarse resolution. This is achieved by recursively subdividing a rectangular phase-space region into four geometrically similar, non-overlapping rectangles, effectively resulting in a quadtree domain decomposition. The recursion stops at a suitable condition, e.g. when reaching a rectangle that contains an integrated PSD smaller than a threshold ϵ , or a maximum recursion depth is reached. $\Psi(q, p)$ is then sampled on an equidistant grid covering this final leaf-rectangle and only these values are stored in memory. An example of the resulting phase-space decomposition is illustrated in Figure 2. In order to evaluate the resulting representation of Ψ at an arbitrary (in general off-grid) point an interpolation scheme based on the function values for the leaf-rectangle containing this point is employed.

Having this efficient data structure at hand the Perron-Frobenius steps needed for the evaluation of Eq. (7) can

Algorithm 1 Perron-Frobenius Steps

- 1: Initialize Ψ_0 as tree-mesh from input, e.g. a smooth function or a particle distribution, as described above
- 2: **for** $n = 1, \dots, N_{BC}$ **do**
- 3: Calculate kicks by projecting Ψ_{n-1} to ρ_{n-1} and solve Poisson's equation to determine $M_{n \leftarrow n-1}[\Psi_{n-1}]$
- 4: Extract an ensemble of points `pts` representative for the shape of Ψ , e.g. corner points of the leafs
- 5: Calculate forward tracked points `pts_fwd` by applying $M_{n \leftarrow n-1}[\Psi_{n-1}]$ to `pts`
- 6: Based on `pts_fwd` initialize coarse forward mesh
- 7: Update forward mesh by sampling $M_{n \leftarrow n-1} \Psi_{n-1}$ and refine/coarsen where necessary, yielding Ψ_n on an optimized tree-mesh
- 8: **end for**

be executed computationally as outlined in Algorithm 1. By first determining a coarse forward mesh which is later adjusted, this algorithm aims to reduce the computation-time intensive tracking of points as much as possible. Adjustment includes the further refinement of rectangles but also the possibility to coarsen them, depending on the local behavior of the PSD. As a result of the assumed continuity of Ψ a clear sign for the need for further refinement is if $\Psi > \epsilon$ on the edge of a leaf-rectangle leading to a non-refined area. A further condition necessary for a successful Perron-Frobenius step that can easily be checked is the conservation of probability $\int_{\Omega \subset \mathbb{R}^2} \Psi d\vec{z} = 1$ within the area Ω covered by the forward mesh.

OUTLOOK

We expect an efficient simulation code based on the proposed method to be a useful tool to evaluate bunch compression schemes of existing accelerators with regard to their susceptibility to the LSC-driven micro-bunching instability, as well as to gain a better understanding of the underlying amplification process, potentially leading to new concepts to mitigate the undesired effects.

REFERENCES

- [1] E.L. Saldin, E.A. Schneidmiller and M.V. Yurkov, *Nucl. Instrum. and Methods A* **528**, 355 (2004).
- [2] Zh. Huang, *ICFA Beam Dynamics Newsletter* **38**, 37 (2005).
- [3] M. Vogt, T. Limberg, D.H. Kuk, in *Proc. EPAC'08*, Genoa, Italy, paper THPC111 (2008).
- [4] M. Clemens, M. Dohlus, S. Lange and G. Pöplau, *internal report DESY TESLA-FEL Report 2009-02* (2009).
- [5] R. Warnock and J. Ellison, *Proc. 2nd ICFA Workshop on High Brightness Beams, UCLA, 1999*, preprint SLAC-PUB-8404 (2000).
- [6] M. Vogt, T. Sen and J.A. Ellison, *Phys. Rev. ST Accel. Beams* **5**, 024401 (2002).